

organization. When this film was reduced back to Ag<sup>II</sup>TNPc (Figure 11b) with hydrazine, the dichroic ratio declined almost to unity, indicating loss of order. A much thinner film (four layers) was used to repeat the liquid-phase experiment, with the same results being obtained.

Thin-film reorganization upon redox sampling undoubtedly involves solvent transfer through the film.<sup>32,33</sup> Thus, the loss of organization upon solvent-phase oxidation, but retention during gas-phase oxidation, may reflect the disruptive effect of such solvent transport in the former case.

**Summary and Conclusions.** Highly ordered well-behaved Ag<sup>II</sup>TNPc(-2) Langmuir-Blodgett films can be codeposited with stearic acid onto suitable substrates, with a deposition ratio of unity. Increasing stearic acid facilitates the transfer of a compact film but decreases the degree of organization of the Ag<sup>II</sup>TNPc(-2) component. The ESR spectra of the mixed Ag<sup>II</sup>TNPc(-2)/SteA films show that aggregation is still occurring, evidence that the stearic acid does not interleave between the Ag<sup>II</sup>TNPc(-2) molecules. Thus, dilute films are likely composed of domains of aggregated Ag<sup>II</sup>TNPc(-2) which are internally ordered, separated

by stearic acid, but with some loss of relative organization between the domains. The presence of the dichroism in the film spectra suggests that each domain consists of Ag<sup>II</sup>TNPc(-2) molecules with their macrocyclic plane tending to face the dipping direction. In the films of higher relative Ag<sup>II</sup>TNPc concentration, each of the domains has a similar orientation, resulting in the anisotropic optical property. The degree of freedom with which the domains orient is dependent upon the relative amount of SteA in the mixture. A larger relative amount of SteA results in a larger degree of freedom for domain orientation and, therefore, worsens the film organization.

Film organization is largely unaffected by electrochemical cycling or by chemical cycling using gaseous chlorine and aqueous hydrazine, but the order is rapidly lost if the film is cycled using a solution chemical oxidant, perhaps due to solvent transport. Retention during electrochemical oxidation in solution shows that different solvent transport and likely anion compensation pathways occur depending upon whether the method of oxidation is chemical or electrochemical. Clearly the detailed mechanisms require further study.

*Acknowledgment.* We are indebted to the Natural Sciences and Engineering Research Council (Ottawa) and the Office of Naval Research (Washington, DC) for financial support.

(32) Bruckenstein, S.; Hillman, A. R. *J. Chem. Phys.* **1988**, *92*, 4837.  
(33) Bruckenstein, S.; Wilde, C. P.; Hillman, A. R. *J. Phys. Chem.* **1990**, *94*, 6458.

## Second Harmonic Generation Studies of Methylene Blue Orientation at Silica Surfaces

Daniel A. Higgins, Shannon K. Byerly, Michael B. Abrams, and Robert M. Corn\*

*Department of Chemistry, University of Wisconsin—Madison, 1101 University Ave., Madison, Wisconsin 53706*  
(Received: September 17, 1990)

The average molecular orientation of methylene blue molecules adsorbed onto a silica substrate is obtained from measurements of the resonant molecular optical second harmonic generation (SHG) from the interface at several wavelengths. A  $\pi$ -electron nonlinear polarizability calculation is used to identify the primary molecular tensor elements responsible for the large nonlinear optical response of the adsorbed methylene blue. The polarization dependence of the SHG signal at three wavelengths is then used to calculate the average dye molecule orientation. Inclusion of the Fresnel coefficients of the interface and the dielectric constant for the methylene blue monolayer at both the fundamental and second harmonic wavelengths is required for the orientation calculation. Phase measurements of the surface nonlinear susceptibility are performed in order to demonstrate the complex nature of the SHG from the interface. The average methylene blue orientation is then determined by using both the polarization dependence and phase measurements of the nonlinear response. The SHG measurements presented here yield an average angle of 58° between the long axis of the methylene blue molecule and the surface normal. Possible methylene blue dimer geometries on the surface are discussed in light of the SHG measurements.

### Introduction

Optical second harmonic generation (SHG) is an inherently surface-sensitive technique for studying the interface between two centrosymmetric media.<sup>1,2</sup> SHG has been employed extensively at a wide variety of surfaces (air-solid, liquid-solid, liquid-air, liquid-liquid) because of its demonstrated submonolayer sensitivity,<sup>3</sup> rapid optical response time,<sup>4</sup> and ability to easily discriminate between surface species and species in the adjacent bulk media.<sup>5</sup> One extensive application of SHG at both liquid and solid surfaces has been the determination of average molecular orientation within the interfacial region.<sup>3-14</sup> For systems where

the SHG from the interface is dominated by the molecular contributions to the surface nonlinear susceptibility, this orientation measurement can be obtained through the analysis of the polarization dependence of the second harmonic response. The average molecular orientation at the surface is obtained by assuming a molecular orientation distribution function and fitting the experimental data with this model.

(1) Shen, Y. R. *The Principles of Nonlinear Optics*; Wiley: New York, 1984.

(2) Shen, Y. R. *Annu. Rev. Phys. Chem.* **1989**, *40*, 327.

(3) (a) Heinz, T. F.; Tom, H. W. K.; Shen, Y. R. *Phys. Rev.* **1983**, *A28*, 1883. (b) Heinz, T. F. Ph.D. Dissertation; University of California, Berkeley, 1982.

(4) Sitzmann, E. V.; Eisenthal, K. B. *J. Phys. Chem.* **1988**, *92*, 4579.

(5) Campbell, D. J.; Higgins, D. A.; Corn, R. M. *J. Phys. Chem.* **1990**, *94*, 3681.

(6) Heinz, T. F.; Chen, C. K.; Ricard, D.; Shen, Y. R. *Phys. Rev. Lett.* **1982**, *48*, 478.

(7) DiLazzaro, P.; Mataloni, P.; DeMartini, F. *Chem. Phys. Lett.* **1985**, *114*, 103.

(8) (a) Hicks, J. M.; Kemnitz, K.; Eisenthal, K. B.; Heinz, T. F. *J. Phys. Chem.* **1986**, *90*, 560. (b) Kemnitz, K.; Bhattacharyya, K.; Hicks, J. M.; Pinto, G. R.; Eisenthal, K. B.; Heinz, T. F. *Chem. Phys. Lett.* **1986**, *131*, 285.

(9) Mazely, T. L.; Hetherington, W. M. III *J. Chem. Phys.* **1987**, *86*, 3640.

(10) Peterson, E. S.; Harris, C. B. *J. Chem. Phys.* **1989**, *91*, 2683.

(11) Dick, B. *Chem. Phys.* **1985**, *96*, 199.

(12) Dick, B.; Gierulski, A.; Marowsky, G.; Reider, G. A. *Appl. Phys. B* **1985**, *38*, 107.

(13) Guyot-Sionnest, P.; Shen, Y. R.; Heinz, T. F. *Appl. Phys.* **1987**, *B42*, 237.

(14) Akstipetrov, O. A.; Akhmediev, N. N.; Baranova, I. M.; Mishina, R. D.; Novak, V. R. *Sov. Phys. JETP* **1985**, *62*, 524.

One of the original surface molecular orientation determinations using SHG was performed by Heinz et al.<sup>6</sup> on dye molecules adsorbed onto silica surfaces. They examined the wavelength and polarization dependence of the second harmonic response from adsorbed rhodamine dyes and estimated the average molecular orientation from their SHG measurements. Subsequent papers have confirmed these orientation measurements at different wavelengths,<sup>7</sup> extended the SHG experiments to other molecules,<sup>3,8-10</sup> and expanded the orientation calculation.<sup>11-14</sup> All of the SHG orientation studies to date have had to make assumptions regarding (i) the dominant molecular nonlinear polarizability tensor elements of the dye molecule, (ii) the linear optical constants of the dye monolayer, and (iii) the orientational distribution function for the adsorbed molecules.

This paper describes the extension and refinement of this methodology and its application to the determination of the average molecular orientation of methylene blue molecules adsorbed onto fused silica substrates. Through the use of multiple wavelengths and additional calculations, several of the assumptions required in the previous orientation measurements are avoided. To understand the nature of the nonlinear molecular response, a Pople-Pariser-Parr (PPP)  $\pi$ -electron calculation of the nonlinear molecular polarizability tensor  $\beta$  is performed. This calculation results in the identification of the dominant polarizability tensor elements in the molecule. For methylene blue, at the wavelengths employed, two different molecular tensor elements are expected to contribute to the SHG response. The individual responses of the adsorbed molecules are then combined to form a surface nonlinear optical response that is characterized by the surface nonlinear susceptibility tensor  $\chi^{(2)}$ .

To correctly ascertain the surface nonlinear susceptibility tensor elements from the SHG polarization data, the incident optical fields at the interface are obtained by the inclusion of the appropriate Fresnel coefficients. In addition, the approximate dielectric constants of the adsorbed monolayer are estimated from a Kramers-Kronig analysis of the monolayer UV-visible absorption spectrum and are included in the calculation. Once the nonlinear susceptibility elements at several wavelengths are known, a molecular orientation distribution function that relates these tensor elements to the molecular polarizability tensor elements can be found. It is the characterization of this molecular orientation distribution function that results in the determination of the average molecular orientation on the surface. Further improvements in the accuracy of the orientation calculation can be obtained by eliminating the assumption that the molecular tensor and monolayer dielectric constants are real. This requires additional experiments that allow for the determination of the relative phases of the different surface tensor elements. These phase relations can then be included in the orientation calculation and new results obtained. For methylene blue molecules, the possibility of dimerization upon adsorption is examined in light of the average molecular orientation. This work is an outgrowth of our previous molecular orientation measurements of methylene blue adsorbed onto sulfur-modified platinum electrodes.<sup>5</sup>

### Sample Preparation and Experimental Apparatus

Optically flat ( $\lambda/4$  and  $\lambda/10$ ) fused silica windows (Esco) were employed as substrates and were thoroughly cleaned prior to monolayer deposition by sequentially sonicating in the following solutions: 10% hot Microcleaner, Millipore-filtered water, 10% hot NaOH, 2% HCl, and hot Millipore-filtered water. The monolayers were then formed by dipping the silica substrate into an ethanolic solution of  $1 \times 10^{-3}$  M methylene blue (Fluka), allowing the solution to slowly flow from the surface upon removal.<sup>15</sup> A UV-visible spectrum of the coated substrate was taken on a Hewlett-Packard 8452A diode array spectrophotometer; representative spectra for methylene blue both as an adsorbed monolayer and in dilute solution are shown in Figure 1. The monolayer spectrum has been smoothed to reduce the errors in

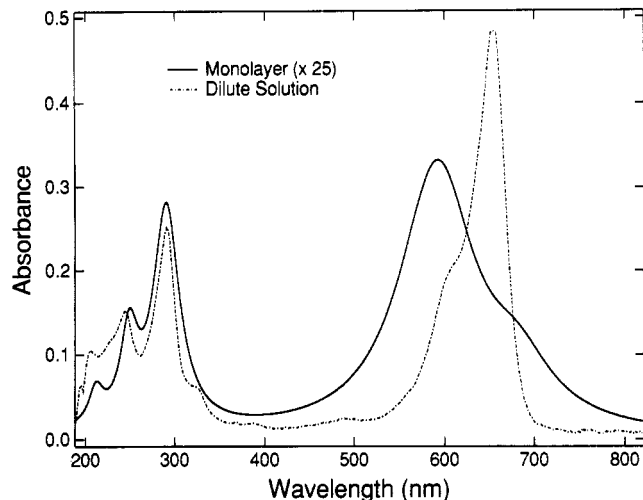


Figure 1. UV-visible absorption spectrum of methylene blue monolayer adsorbed onto a silica substrate (—) and a  $5 \times 10^{-6}$  M solution of methylene blue in ethanol (---). The monolayer spectrum has been smoothed for use in a Kramers-Kronig analysis.

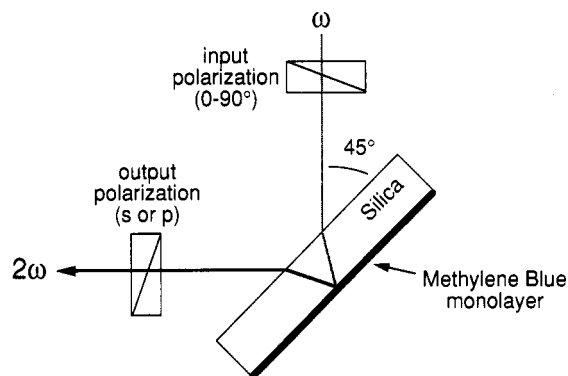


Figure 2. Experimental geometry for the SHG orientation measurements.

the Kramers-Kronig analysis (see below). From the absorbance of the monolayer and the molar absorptivity of the dilute solution spectrum, an approximate surface density of  $5 \times 10^{13}$  molecules/cm<sup>2</sup> was calculated. Lower surface densities could be obtained by varying the solution concentration. Note also in Figure 1 that the monolayer spectrum is blue-shifted by 1500 cm<sup>-1</sup> from the dilute solution spectrum. This blue-shifted peak was observed for all monolayers prepared from solutions of  $2.5 \times 10^{-4}$  M or higher. Below that concentration an absorption peak at 650 nm dominated the spectrum of the monolayer. Since the position of the blue-shifted absorption band did not change with surface concentration, we attribute this absorption to the presence of methylene blue dimers adsorbed onto the surface.<sup>10</sup>

The experimental apparatus employed for the orientation measurements is similar to that described previously.<sup>5,16</sup> For the SHG measurements the dipped silica substrate was cleaned on one side and used as the entrance window of a nitrogen-purged cell. Pulses of light (10-ns pulse width, 10-Hz repetition rate) at either 532, 585, or 615 nm were focused through the window at an incident angle of 45° (corresponding to an incident angle of approximately 30° on the back surface) onto the monolayer with a typical surface energy density of 5 mJ cm<sup>-2</sup> (Figure 2). The polarization of the incident fundamental beam was varied continuously from 0 (p-polarized) to 90° (s-polarized) by a broadband  $\lambda/2$  plate/polarizer (Special Optics) combination. The reflected second harmonic light from the monolayer was collected and sent through a second polarizer (Karl Lambrecht, 10<sup>-5</sup> extinction ratio) set to pass either s-polarized or p-polarized light from the surface. Appropriate UV-passing filters and a 0.175-m monochromator were used to filter out any reflected fundamental

(15) Garoff, S.; Stephens, R. B.; Hanson, C. D.; Sorenson, G. K. *Chem. Phys. Lett.* **1982**, *41*, 257.

(16) Campbell, D. J.; Corn, R. M. *J. Phys. Chem.* **1988**, *92*, 5796.

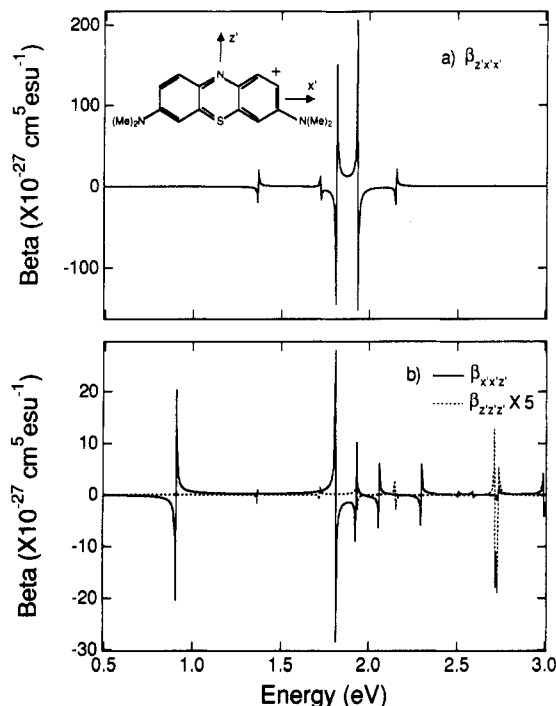


**Figure 3.** Real components of the  $\pi$ -electron molecular nonlinear polarizability calculation for methylene blue: (a)  $\beta_{z'x'x'}$ ; (b)  $\beta_{x'x'x'}$  (—) and  $\beta_{z'z'z'} \times 5$  (---). The tensor elements  $\beta_{z'x'x'}$ ,  $\beta_{x'x'x'}$ , and  $\beta_{z'z'z'}$  are defined with respect to the molecular axes depicted in the figure.

light, and the SHG from the surface was detected with a cooled photomultiplier tube, the output of which was amplified and then averaged with a boxcar averager.

The relative phases of the various elements of the surface nonlinear susceptibility were measured by introducing a second source of SHG into the experiment. This was accomplished by placing a thin z-cut quartz crystal in the path of the beam reflected from the silica surface. Since the SHG from the silica surface is very nearly collinear with the reflected fundamental beam, the SHG generated in the z-cut quartz will interfere with the SHG generated by the monolayer of methylene blue. Thus, by selecting the appropriate input and output polarizations and translating the z-cut quartz parallel to the beam path, interference patterns were produced that provided for the direct determination of the relative phases of the surface susceptibility elements. This method has been discussed in detail elsewhere.<sup>8b,17</sup>

The SHG signal from the monolayer was found to increase monotonically as a function of methylene blue concentration in solution until it leveled off at approximately  $1 \times 10^{-3}$  M. The absorption spectrum of this monolayer is plotted in Figure 1; at this concentration, polarization curves for the s-polarized and p-polarized second harmonic response were obtained from the methylene blue monolayer at the three wavelengths mentioned above. The phase measurements were performed on these same surfaces at 615 nm. The magnitude of the SHG signal from this monolayer was approximately 1500 times the SHG signal obtained from a surface prepared with  $1 \times 10^{-4}$  M methylene blue. This intense doubly resonant response from the dye molecules, which arises from both the fundamental and second harmonic wavelengths being nearly resonant with strong electronic transitions in the molecules, eliminates any possibility of interference from the second harmonic response of the substrate.

### Theoretical Calculations

**Molecular Nonlinear Polarizability Calculation.** The magnitude and polarization dependences of the resonant SHG response obtained from the adsorbed methylene blue monolayer depend upon (i) the average molecular orientation on the surface and (ii) the

intrinsic nonlinear optical response of the adsorbed molecules. This latter property is described by the molecular nonlinear polarizability tensor  $\beta$ . With use of perturbation theory, the components of  $\beta$  can be expressed in terms of the molecular wave functions;<sup>5,9,18,19</sup> for a small number of molecules, a nonlinear polarizability calculation has been performed by using an all-valence electron SCF-CI LCAO wave function calculation.<sup>20</sup> However, for most conjugated aromatic molecules like methylene blue, it is reasonable to assume that the  $\pi$ -electronic structure is the sole contributor to the molecular nonlinear polarizability. For these molecules, an intermediate level of calculation can be employed<sup>19</sup> in which the Pople-Pariser-Parr (PPP) method<sup>21</sup> is used to calculate the  $\pi$ -electron wave functions. A result of the PPP approximation is that the nonlinear optical response must lie in the aromatic plane since both the dipole moment and the transition dipole moments all lie in the plane of the  $\pi$ -electron system.<sup>19</sup> The elements of the nonlinear polarizability tensor can then be expressed in terms of the molecular wave functions as<sup>18</sup>

$$\beta_{ijk} + \beta_{ikj} = \frac{-e^3}{4\hbar^2} \sum_{n'n} (r_{gn}^j r_{n'n}^k r_{gn}^i + r_{gn}^k r_{n'n}^i r_{gn}^j) \times \left( \frac{1}{(\omega_{n'g} - \omega + i\Gamma_{n'g})(\omega_{ng} + \omega - i\Gamma_{ng})} + \frac{1}{(\omega_{n'g} + \omega + i\Gamma_{n'g})(\omega_{ng} - \omega - i\Gamma_{ng})} \right) + (r_{gn}^j r_{n'n}^i r_{gn}^k + r_{gn}^k r_{n'n}^j r_{gn}^i) \times \left( \frac{1}{(\omega_{n'g} + 2\omega - i\Gamma_{n'g})(\omega_{ng} + \omega - i\Gamma_{ng})} + \frac{1}{(\omega_{n'g} - 2\omega - i\Gamma_{n'g})(\omega_{ng} - \omega - i\Gamma_{ng})} \right) + (r_{gn}^j r_{n'n}^k r_{gn}^i + r_{gn}^k r_{n'n}^j r_{gn}^i) \left( \frac{1}{(\omega_{n'g} - \omega + i\Gamma_{n'g})(\omega_{ng} - 2\omega + i\Gamma_{ng})} + \frac{1}{(\omega_{n'g} + \omega + i\Gamma_{n'g})(\omega_{ng} + 2\omega + i\Gamma_{ng})} \right) \quad (1)$$

where  $r_{nn}^j$  is the dipole matrix element  $\langle \phi_n | \mu_j | \phi_n \rangle$ ;  $\hbar\omega_{ng}$  is the difference in energy between the excited state  $n$  and the ground state;  $\Gamma_{ng}$  is the lifetime of the  $n$ th state, and  $\omega$  is the frequency of the applied field. For molecules with  $C_{2v}$  symmetry (such as methylene blue) there are only three nonzero  $\beta$  tensor elements:  $\beta_{x'x'x'} = \beta_{x'z'z'}$ ,  $\beta_{y'z'z'}$ , and  $\beta_{y'y'y'}$ , where the molecular nonlinear polarizability elements are defined with respect to the symmetry axis of the molecule as shown in Figure 3. Terms such as  $\beta_{y'y'y'}$  and  $\beta_{y'z'z'}$  must be zero since the dipole moment and transition dipoles are all assumed to lie in the molecular plane which is perpendicular to the molecular  $y'$  axis.

The lifetime broadening terms  $\Gamma_{ng}$  are included in eq 1 to avoid having the tensor elements diverge as resonance is approached. The exact values of these lifetimes are difficult to estimate and are all arbitrarily set to 1 ns in our calculations (a reasonable lifetime for molecular electronic states). A lower limit of 10 fs for the excited-state lifetimes can be obtained from the widths of the absorption peaks in the UV-visible spectrum; however, this method of estimation neglects any inhomogeneous contributions to the broadening of the peaks. A nonlinear polarizability calculation using this lower lifetime limit yielded results qualitatively similar to those obtained by using lifetimes of 1 ns. The variations inherent in these calculations will not affect the analysis of the experimental data below, since these results are used not in a

(18) Ward, J. F. *Rev. Mod. Phys.* **1965**, *37*, 1.

(19) DeQuan, L.; Ratner, M. A.; Marks, T. J. *J. Am. Chem. Soc.* **1988**, *110*, 1707.

(20) Lalama, S. J.; Garito, A. F. *Phys. Rev.* **1979**, *A20*, 1179.

(21) (a) Pople, J. A. *Trans. Faraday Soc.* **1953**, *49*, 1375. (b) Pariser, R.; Parr, R. G. *J. Chem. Phys.* **1953**, *21*, 466.

(17) Byerly, S. B.; Higgins, D. A.; Abrams, M. B.; Corn, R. M., manuscript in preparation.

quantitative manner but only qualitatively to determine the relative importance of the various  $\beta$  tensor elements.

The calculated nonlinear polarizability elements for methylene blue are shown as a function of energy in Figure 3. To facilitate plotting, energies within 0.0025 eV of an excited state are omitted. The excited-state energies of the methylene blue wave functions obtained by the PPP method for this calculation have been listed previously.<sup>5</sup> In the region of the first excited state at 1.8 eV, the molecular polarizability elements  $\beta_{xxx}$  and  $\beta_{xyx}$  are significant and the  $\beta_{yxx}$  tensor element is relatively small and can be neglected. Most of the previous SHG measurements on dye molecules similar to methylene blue have assumed a single dominant tensor element  $\beta_{xxx}$ .<sup>6</sup> Since the PPP calculations are accurate in energy to about 10% and will shift depending on the molecular environment, the exact contribution of each tensor element is difficult to calculate. The inaccuracies in this theoretical calculation prevent these results from being used in a quantitative manner. However, the relative contributions of  $\beta_{xxx}$  and  $\beta_{xyx}$  can be experimentally determined from the polarization dependence and phase measurements of the SHG signal (see below). By obtaining SHG measurements from several wavelengths in this region where  $\beta_{xxx}$  and  $\beta_{xyx}$  contribute to a varying extent, one can obtain a series of polarization measurements which should all be described by a single molecular orientation distribution.

**Surface Nonlinear Susceptibility Tensor Measurements.** When adsorbed to a surface, a monolayer of molecules collectively responds to an incident laser light field to create an induced surface nonlinear optical response that can be described by the surface nonlinear susceptibility tensor  $\chi^{(2)}$ .<sup>1</sup> Thus surface nonlinear susceptibility leads to the generation of light at the surface at frequency  $2\omega$  with intensity  $I(2\omega)$ . The observed intensity can be related to  $\chi^{(2)}$  by

$$I(2\omega) = \frac{32\pi^3\omega^2 \sec^2 \theta_{2\omega}}{c^3 A} |e(2\omega) \cdot \chi^{(2)} : e(\omega) e(\omega)|^2 I^2(\omega) \quad (2)$$

where  $I(\omega)$  is the intensity of input laser light,  $\theta_{2\omega}$  is the angle from the surface normal at which the SHG signal occurs, the vectors  $e(\omega)$  and  $e(2\omega)$  describe the polarization and Fresnel factors for the fundamental and second harmonic light fields at the surface.  $A$  is the illuminated surface area, and all other symbols have their usual meaning. This equation has been derived by Heinz<sup>3b</sup> and by Mizrahi and Sipe.<sup>22</sup>

In general, the surface nonlinear susceptibility tensor is a sum of electric-dipole contributions from the adsorbate and the silica surface as well as higher order contributions from the adjacent bulk media. In the case of a nonconducting material such as silica, the contributions to  $\chi^{(2)}$  in the absence of dye molecule absorption are relatively small. By choosing a wavelength where the dye molecule at the interface has transitions in resonance with both the fundamental and the second harmonic light, one ensures that the surface nonlinear susceptibility arises solely from contributions of the adsorbed monolayer.

To determine  $\chi^{(2)}$ , one must first ascertain the vectors  $e(2\omega)$  and  $e(\omega)$  for the particular SHG experiment. The geometry of the SHG experiments employed here is shown in Figure 2. For fused silica, a nonabsorbing substrate, the Fresnel factors are real. The components of these vectors can easily be derived by following the formalism of Mizrahi and Sipe,<sup>22</sup> who assume that the driving fields are in the silica and the second harmonic light is generated in air. The three components for light at the fundamental wavelength are given by

$$\begin{aligned} e_x(\omega) &= t_1^{\parallel}(\omega)[1 - r_2^{\parallel}(\omega)] \cos \theta_{\omega} \\ e_y(\omega) &= t_1^{\perp}(\omega)[1 + r_2^{\perp}(\omega)] \\ e_z(\omega) &= t_1^{\parallel}(\omega)[1 + r_2^{\parallel}(\omega)] \sin \theta_{\omega} \end{aligned} \quad (3)$$

where  $\theta_{\omega}$  is the angle of incidence as measured inside the silica. The Fresnel coefficients  $t_1^{\parallel}$  and  $t_1^{\perp}$  are for transmission of light (polarized parallel and perpendicular to the plane of incidence,

respectively) through the first interface while  $r_2^{\parallel}$  and  $r_2^{\perp}$  are for reflection of light from the second interface. Similarly, for the output light at  $2\omega$

$$\begin{aligned} e_x(2\omega) &= -t_1^{\parallel}(2\omega)t_2^{\parallel}(2\omega) \cos \theta_{2\omega} \\ e_y(2\omega) &= t_1^{\perp}(2\omega) t_2^{\perp}(2\omega) \\ e_z(2\omega) &= t_1^{\parallel}(2\omega)t_2^{\parallel}(2\omega) \sin \theta_{2\omega} \end{aligned} \quad (4)$$

where  $\theta_{2\omega}$  is the angle at which the second harmonic is generated in air. For p-polarized light the electric field is parallel to the plane of incidence ( $x$ - $z$  plane), so  $e_x$  and  $e_z$  are nonzero and  $e_y$  is zero. For s-polarized light, only the component perpendicular to the plane of incidence,  $e_y$ , is nonzero.

It is assumed that the methylene blue molecules adsorbed onto the silica surface are randomly distributed in terms of rotation around the surface normal. This assumption can be checked by verifying that the SHG signal has no azimuthal angle dependence. For such a case,  $\chi^{(2)}$  has only three nonzero tensor elements:  $\chi_{xxx} = \chi_{xzz}$ ,  $\chi_{zxx}$ , and  $\chi_{zzz}$ . The intensity of the s-polarized and p-polarized SHG signal can be directly related to these elements:<sup>5</sup>

$$I_s \propto |a_1 \sin 2\gamma \chi_{xxx}|^2 \quad (5)$$

$$I_p \propto |\cos^2 \gamma (a_2 \chi_{xxx} + a_3 \chi_{zxx} + a_4 \chi_{zzz}) + \sin^2 \gamma a_5 \chi_{xxx}|^2 \quad (6)$$

where  $\gamma$  is the polarization angle of the incident light ( $\gamma = 0^\circ$  for p-polarized light and  $\gamma = 90^\circ$  for s-polarized light), and the  $a_i$  terms are products of the components of  $e(\omega)$  and  $e(2\omega)$ :

$$\begin{aligned} a_1 &= e_y(\omega) e_z(\omega) e_y(2\omega) e_z(2\omega) / \epsilon(\omega) \\ a_2 &= 2e_x(\omega) e_z(\omega) e_x(2\omega) e_z(2\omega) / \epsilon(\omega) \\ a_3 &= |e_x(\omega)|^2 e_z(2\omega) / \epsilon(2\omega) \\ a_4 &= |e_z(\omega)|^2 e_x(2\omega) e_z(2\omega) / \{\epsilon^2(\omega) \epsilon(2\omega)\} \\ a_5 &= |e_y(\omega)|^2 e_z(2\omega) / \epsilon(2\omega) \end{aligned} \quad (7)$$

These values of  $a_1$ - $a_5$  differ from those employed previously<sup>5</sup> in that they include the values of the dielectric constants of the monolayer  $\epsilon(\omega)$  and  $\epsilon(2\omega)$  and the substrate  $\epsilon_s(\omega)$ . As discussed by Guyot-Sionnest et al.,<sup>13</sup> the elements of  $\chi^{(2)}$  in eqs 5 and 6 are actually effective values that neglect these dielectric constants.

Approximate values for the monolayer dielectric constant can be calculated through the use of the UV-visible absorption spectrum of the sample. The complex dielectric constant of the thin film is given by  $\epsilon(\omega) = [\eta(\omega) + i\kappa(\omega)]^2$ , where  $\eta(\omega)$  is the refractive index and  $\kappa(\omega)$  is the extinction coefficient of the monolayer. The wavelength dependence of  $\kappa(\omega)$  can be determined directly from the UV-visible absorbance  $A(\omega)$ :<sup>23</sup>

$$\kappa(\omega) = cA(\omega)/2\omega z \quad (8)$$

where  $z$  is the thickness of the monolayer. The value for this thickness is approximate and is estimated to be 1 nm as suggested from ellipsometric measurements.<sup>12</sup> The values for  $\eta(\omega)$  can be calculated from  $\kappa(\omega)$  through the use of the Kramers-Kronig relation<sup>23</sup>

$$\eta(\omega) - 1 = \frac{2}{\pi} P \int_0^{\infty} \frac{\omega' \kappa(\omega')}{\omega'^2 - \omega^2} d\omega' \quad (9)$$

where  $P$  signifies that the Cauchy principal value of the integral is taken. The values calculated for  $\eta(\omega)$  will only be approximate since  $\kappa(\omega)$  is not available for all frequencies; however, absorption peaks far from the desired wavelengths will not significantly affect the results. The results of the calculation of  $\eta(\omega)$  and  $\kappa(\omega)$  for the methylene blue monolayer are shown in Figure 4. From this calculation, the approximate dielectric constants were estimated at the three wavelengths employed in the SHG studies and are given in Table I. These values can be assumed good to within 25%. With these estimates of  $\epsilon(\omega)$  and  $\epsilon(2\omega)$ , the values of  $a_1$ - $a_5$ ,

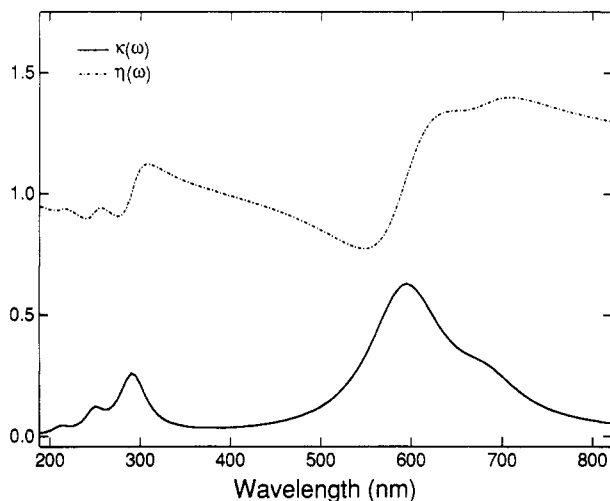


**Figure 4.** Kramers-Kronig analysis of the methylene blue monolayer adsorption spectrum. The dielectric constant  $\epsilon(\omega)$  is defined as the square of the complex index of refraction  $\eta(\omega) + i\kappa(\omega)$  and is required in the molecular orientation calculation.

**TABLE I: SHG Orientation Calculation Results for Methylene Blue Molecules Adsorbed onto Silica Surfaces<sup>a</sup>**

$\lambda$ , nm	$\epsilon(\omega)^b$	$\epsilon(2\omega)^b$	$\chi_{xxx}/\chi_{zzz}$	$\chi_{zzz}/\chi_{xxx}$	$\beta_r$	$\xi$ , deg
532	0.7	0.9	1.06	2.72	1.03	64.3
585	1.4	1.1	0.48	2.59	0.77	62.0
615	2.1	1.5	0.37	3.05	0.75	60.5
615	$1.6 + i1.4$	$1.4 + i0.2$	0.37	2.05	$0.94^c$	57.5

<sup>a</sup>  $\xi$  is the average angle between the transition dipole moment ( $x'$  axis) and the surface normal. <sup>b</sup> Variations of 25% in the dielectric constant lead to errors in  $\xi$  of  $\approx 3^\circ$ . <sup>c</sup> The phasing of  $\beta_{xxx}$  relative to  $\beta_{zzz}$  is  $\approx +40^\circ \pm 10^\circ$ .

can be calculated, and the elements of  $\chi^{(2)}$  can be determined from the SHG polarization curves (eqs 5 and 6).

**Molecular Orientation Distribution Function.** Once the elements of the surface nonlinear susceptibility  $\chi^{(2)}$  have been determined, they can be related to the elements of the molecular nonlinear polarizability  $\beta$  by the molecular orientation distribution function. This mathematical relationship can be described as the average of the product of three direction cosines:

$$\chi_{IJK} = N_s \sum_{ijk} \langle R_{Ii} R_{Jj} R_{Kk} \rangle \beta_{ijk} \quad (10)$$

where  $N_s$  is the surface concentration of dye molecules, and  $R_{Ii}$  is the direction cosine between the macroscopic and molecular Cartesian axes ( $I$  and  $i$  respectively), and the brackets denote an average over all of the molecules on the surface. Peterson and Harris have reduced this distribution function to one based only on the angle  $\xi$  between the transition dipole moment along the  $x'$  axis and the surface normal,<sup>10</sup> as is shown in Figure 5. Although this analysis was originally presented for the case of a single dominant tensor element,  $\beta_{zzz}$ , it remains valid when both  $\beta_{zzz}$  and  $\beta_{xxx}$  contribute to the molecular nonlinear response. To arrive at the results obtained by Peterson and Harris, two initial assumptions must be made. First, as noted above, it is assumed that there is no preferential molecular orientation with respect to rotation about the surface normal, and second, the molecules are all assumed to lie on the surface in a single orientation with respect to the remaining degrees of freedom. Through the application of this methodology, the average molecular orientation can be determined from a fit of the experimental data.

## Results and Discussion

The input polarization dependence of the p-polarized and s-polarized SHG signals from the methylene blue monolayer are shown in parts a-c of Figure 6 for the fundamental wavelengths of 532, 585, and 615 nm, respectively. Each polarization curve was normalized to the maximum second harmonic response observed at that particular wavelength. The relative intensities of

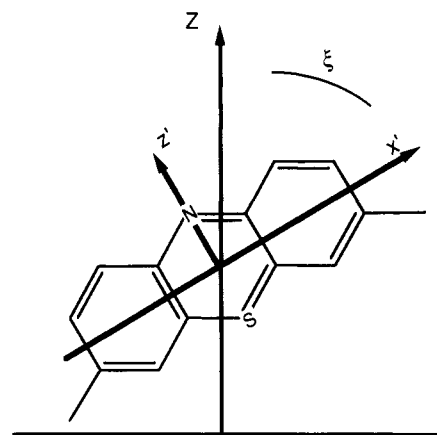


**Figure 5.** Relation between the molecular axes  $x'$ ,  $y'$ , and  $z'$  and the surface axes  $X$ ,  $Y$ , and  $Z$  for an adsorbed methylene blue molecule. The orientation measurements assume that there is no preferential molecular orientation with respect to rotation about the surface normal.

the maximum SHG signal observed at 532, 585, and 615 nm were approximately 1:5:2. These relative intensities agree with the doubly resonant behavior expected from the maxima at 592 and 292 nm in the methylene blue monolayer absorption spectrum (Figure 1).

The sets of polarization curves in Figure 6 were fit to eqs 5 and 6 to obtain values for  $\chi_{xxx}$ ,  $\chi_{zzz}$ , and  $\chi_{zzx}$  at each of the three wavelengths. As an initial approximation, all values used in the calculations were assumed to be real. The apparent validity of this assumption is demonstrated in Figure 7, where the effects of various phase shifts between the tensor elements on the appearance of the  $I_p$  curve at 615 nm are shown. To within experimental error, none of the three  $I_p$  curves deviate from that which is expected when little or no phase difference occurs between the tensor elements. Thus, all of the surface tensor elements are assumed to be real. The remaining sign ambiguities in the surface tensor elements can be eliminated by finding an average molecular orientation that fits the SHG data at all three wavelengths.

As stated above, in previous SHG studies, a single molecular nonlinear polarizability tensor element was assumed to dominate the molecular response.<sup>6</sup> None of the data obtained in the methylene blue experiments could be fit by using the assumption of either  $\beta_{zzz}$  or  $\beta_{xxx}$  as single dominant tensor elements, thus confirming the results of the theoretical calculations. Relaxing this constraint in order to allow for simultaneous contributions from both of these tensor elements allows for the data to be fit. The following equation relating the ratio of the molecular nonlinear polarizability tensor elements,  $\beta_r$ , to the experimental results can be derived from eq 10:

$$\beta_r = \frac{\beta_{zzz}}{\beta_{xxx}} = \frac{\chi_{zzz} + 2\chi_{zzx}}{\chi_{zzz} + 2\chi_{zzx}} \quad (11)$$

Once this ratio is determined, the angle  $\xi$  can be obtained from

$$\cos^2 \xi = (1 + 2\beta_r)^{-1} \frac{\chi_{zzz}}{\chi_{zzz} + 2\chi_{zzx}} \quad (12)$$

The derivation of this relationship requires the assumptions about the molecular orientation distribution function that were discussed above. The experimentally determined  $\beta$  ratios and molecular angles for the three wavelengths are listed in Table I. The SHG measurements at the three wavelengths can all be fit with molecular orientation models of  $\xi \approx 62^\circ$ .

Although the experimental data could be fit quite well with real tensor elements, this assumption can be avoided by performing phase measurements on the nonlinear response of the monolayer. The fact that both the fundamental and second harmonic wavelengths are nearly resonant with electronic transitions in the methylene blue monolayer suggests that both the dielectric constant of the monolayer and the molecular nonlinear polarizability of the molecules may have nonnegligible imaginary components.

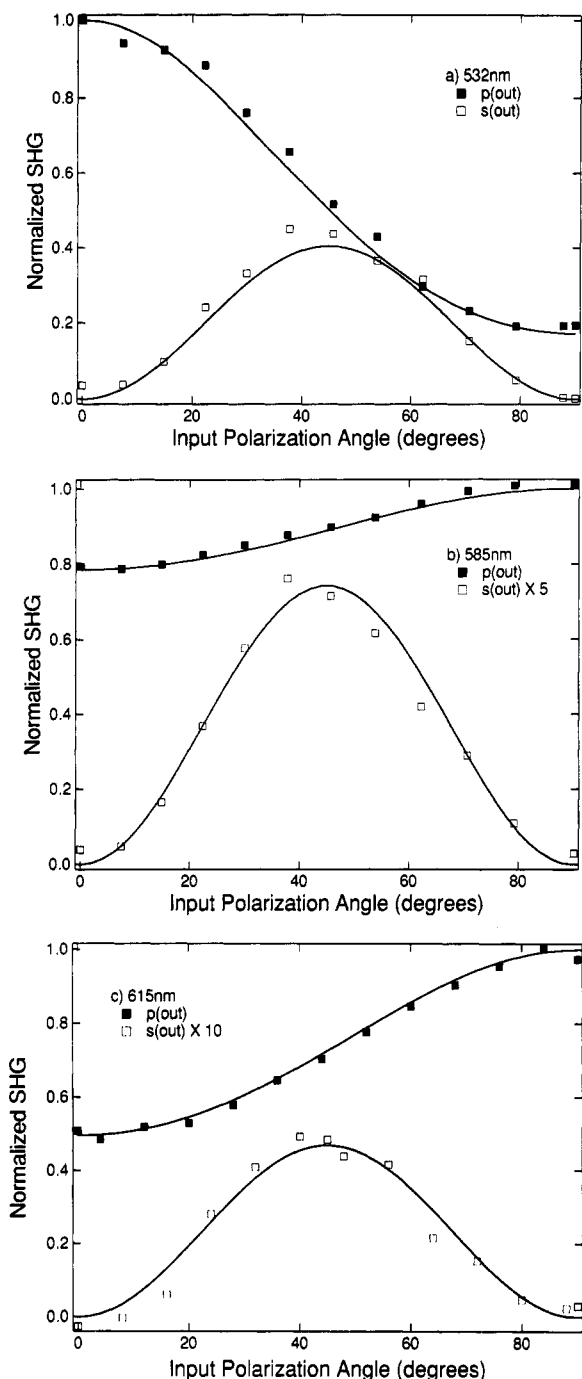


**Figure 6.** P-polarized (filled squares) and s-polarized (open squares) SHG from the methylene blue monolayer as a function of input polarization at three wavelengths: (a) 532; (b) 585; (c) 615 nm. The SHG signal is normalized to the maximum second harmonic response observed at that particular wavelength. The relative intensities of the maximum SHG signal observed at 532, 585, and 615 nm were approximately 1:5:2. The input polarization angle is defined as  $0^\circ$  for p-polarized fundamental light and  $90^\circ$  for s-polarized fundamental light. The solid lines are the theoretical fits used to determine the values of  $\chi_{xxx}$ ,  $\chi_{xxz}$ , and  $\chi_{zzz}$  at the three wavelengths, assuming that all values are real.

This should result in measurable phase shifts between the various surface susceptibility elements. These phase shifts can be observed experimentally through the use of the interference technique described above. The nonlinear polarization measured at  $I_p(\gamma=45^\circ)$  was found to have an average phase shift for several experiments of  $-42^\circ \pm 10^\circ$  relative to the nonlinear polarization measured at  $I_p(\gamma=90^\circ)$  (see eqs 5 and 6). An average phase shift of  $+22^\circ \pm 10^\circ$  was found for the nonlinear polarization at  $I_p(\gamma=0^\circ)$  relative to that at  $I_p(\gamma=90^\circ)$ . The experimental results of the phase measurements at 615 nm are shown in Figure 7 along with the effects of various phase shifts on the appearance of the

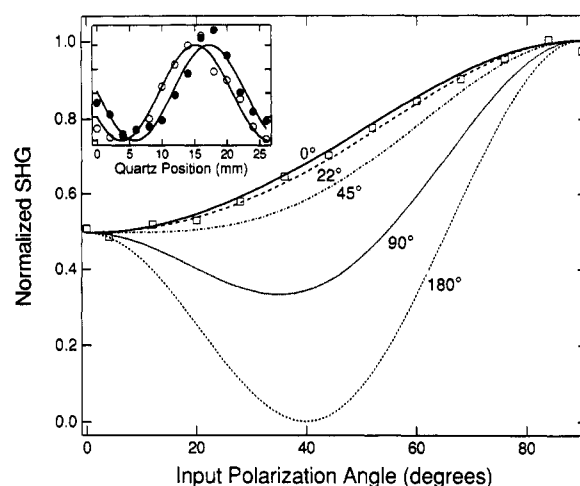


**Figure 7.** P-polarized SHG from the methylene blue monolayer as a function of input polarization for 615 nm. The effects of various phase shifts between the nonlinear polarization at  $\gamma = 0^\circ$  and  $\gamma = 90^\circ$  are shown. The inset shows typical experimental results for this phase shift obtained with the z-cut quartz crystal interference method discussed in the text. For the inset, the open circles and filled circles denote the data for  $\gamma = 0^\circ$  and  $\gamma = 90^\circ$ , respectively. The results for several experiments indicate an average phase shift of  $+22^\circ \pm 10^\circ$ .

p-polarized SHG curve. These phase shifts can be included in the orientation calculation and result in a minor modification of the average orientation.<sup>17</sup> Specifically, the average orientation is found to change from  $\xi = 62^\circ$  to  $\xi = 58^\circ$  when the phase measurements are included in the analysis. These results are presented in Table I.

Further information on the orientation of the molecules relative to one another can be obtained by including the optical absorption measurements in the orientation analysis. The UV-visible absorption spectrum of the monolayer shows a pronounced concentration-independent shift of the first absorption band relative to that in solution, thus suggesting the presence of methylene blue dimers in the monolayer. By using the average molecular angle determined from the SHG experiments along with the UV-visible absorption data, one can suggest possible geometries for the adsorbed methylene blue dimers on the silica surface. As mentioned above, in the case of methylene blue, a  $1500\text{-cm}^{-1}$  blue shift of the first absorption band is observed upon adsorption. This result implies a dimerization of the methylene blue molecules in which their  $x'$  axes must lie parallel to each other and perpendicular to the intermolecular vector. The simultaneous use of SHG data and band shifts in the optical absorption spectrum upon adsorption to a substrate have also been explored by Peterson and Harris for the rhodamine B molecule.<sup>10</sup>

## Conclusions

In summary, the average molecular orientation of methylene blue adsorbed onto a fused silica substrate has been calculated from the polarization dependence of the doubly resonant second harmonic response at several wavelengths. The results presented here yield an average angle of  $58^\circ$  between the long axis of the methylene blue molecule and the surface normal. Unlike previous SHG orientation measurements, contributions from more than one molecular nonlinear polarizability tensor element are found to contribute to the SHG from the adsorbed dye molecules. These elements can be identified through  $\pi$ -electron molecular nonlinear polarizability calculations. It was also shown that the assumptions of a real dielectric constant for the monolayer of molecules and a real molecular nonlinear polarizability are not completely valid. However, the inclusion of the results of relative phase measurements in the orientation calculation lead to only a small change in the molecular orientation results for methylene blue.

To perform the orientation calculations, estimates of the dielectric constants for the monolayer at the fundamental and second harmonic wavelengths were obtained from a Kramers-Kronig analysis of the optical absorption spectrum. This spectrum also

revealed a concentration-independent blue shift of the first absorption band that indicated the existence of methylene blue dimers in the monolayer. A simple model of methylene blue dimer adsorption which fits the SHG orientation data was suggested. Finally, it has been demonstrated that the inclusion of multiple elements of  $\beta$ , monolayer dielectric constants, and phase mea-

surements all contribute to the improvement of the SHG orientation calculation.

*Acknowledgment.* We gratefully acknowledge the support of the National Science Foundation in these studies.

Registry No. Silica, 60676-86-0; methylene blue, 61-73-4.

## Reflectance Spectroscopic Studies of the Cation Radical and the Triplet of Pyrene on Alumina

Surapol Pankasem and J. Kerry Thomas\*

Department of Chemistry and Biochemistry, University of Notre Dame, Notre Dame, Indiana 46556  
(Received: November 20, 1990; In Final Form: February 7, 1991)

The triplet state and the cation radical of pyrene are produced on excitation of pyrene adsorbed on  $\gamma$ -alumina. The characteristic absorption spectra of these two alumina bound transients are similar to those in solution and exhibit absorption bands at 415 and 450 nm for the triplet and the cation, respectively. The triplet state decays exponentially with a lifetime of 5.1 ms, while the cation decays in a more complicated fashion which can be described by a Gaussian distribution of the logarithm of the rate constant at various adsorption sites. Movement of ferrocene to the triplet state on the surface quenches the triplet via energy transfer. The bimolecular quenching rate constants of pyrene triplet by ferrocene are  $3.31 \times 10^{11}$ ,  $2.63 \times 10^{11}$ , and  $2.20 \times 10^{11} \text{ m}^2 \text{ mol}^{-1} \text{ s}^{-1}$  for alumina at pretreatment temperatures of 130, 250, and 350 °C, respectively. Pretreatment of the alumina surface at high temperature decreases the number of surface hydroxyl groups. These bind adsorbed molecules less strongly than the acidic sites formed at the high pretreatment temperature. Hydration of the surface by small amounts of coadsorbed water increases the number of surface hydroxyl groups and enhances the degree of dynamic quenching. The formation of the cation radical of pyrene on alumina is a two-photon process, and the cation radical is quenched dynamically by ferrocene. The studies clearly distinguish the role played by heat activation of alumina on the diffusion and rates of photoinduced process on the surfaces. A comparison with similar results on silica shows that adsorbed molecules are less mobile on alumina.

### Introduction

Molecular dynamics of adsorbed molecules on metal oxides have received attention for many decades. The technique of fluorescence probing has been used to investigate the diffusion of adsorbed fluorescing polyaromatic hydrocarbons on silica and alumina.<sup>1-4</sup> The diffuse reflectance laser photolysis technique<sup>5</sup> enables one to monitor triplet-triplet absorption of adsorbed hydrocarbons on these oxides.<sup>6-8</sup>

The literature indicates some disagreement regarding the effect of oxide pretreatment temperature on the diffusion processes on silica surfaces. A triplet-triplet annihilation study of acridine adsorbed on silica indicated that higher pretreatment temperatures cause the acridine to diffuse more slowly as the number of silanol groups is reduced. It was also observed that acridine does not move on an alumina surface on the time scale of the experiments.<sup>6</sup> On the other hand, fluorescence photobleaching studies of tetracene<sup>9</sup> showed that the diffusion increased when the silica was pretreated at high temperatures.

This paper presents the transient reflectance laser photolysis study of pyrene adsorbed on  $\gamma$ -alumina. Photolysis of adsorbed pyrene yields the triplet state and the cation radical. With low-temperature pretreated alumina surfaces, the energy transfer from the triplet state of pyrene to ferrocene, i.e., the triplet quenching, is dynamic in nature. It is believed that this is the first report on diffusion on alumina by diffuse reflectance laser photolysis. The bimolecular quenching rate constants on alumina surfaces at different pretreatment temperatures indicate that the mobility of the adsorbed species decreases with increasing pretreatment temperature. The difference in mobility is attributed to the relative strength of solute binding to the hydroxyl layer on the surface compared to binding at the Lewis acid sites. Higher pretreatment temperatures increases the surface Lewis acid sites which leads

TABLE I: Specific Properties of  $\gamma$ -Alumina at Various Pretreatment Temperatures ( $T_p$ )

$T_p$ , °C	surf. area, $\text{m}^2/\text{g}$	OH groups, <sup>a</sup> $\text{cm}^{-2}$	Lewis acid sites, <sup>b</sup> $\text{cm}^{-2}$
130	200	$11.5 \times 10^{14}$	$0.8 \times 10^{14}$
250	200	$7.8 \times 10^{14}$	$1.6 \times 10^{14}$
350	200	$6.2 \times 10^{14}$	$2.1 \times 10^{14}$
450	200	$4.6 \times 10^{14}$	$2.4 \times 10^{14}$
750	200	$1.3 \times 10^{14}$	$3.0 \times 10^{14}$

<sup>a</sup>The numbers were taken from ref 26. <sup>b</sup>Calculated from the amount of the cation radical of *N,N,N',N'*-tetramethylbenzidine produced similar to that described in ref 12.

to increasing yield of ferrocenium ions. The quenching process on the surfaces of high pretreatment temperatures therefore switches from dynamic to static in nature.

### Experimental Section

**Materials.** Pyrene (Aldrich Chemical Co.) was purified by silica gel/cyclohexane column chromatography. Ferrocene (Aldrich Chemical Co.) was purified by vacuum sublimation. Cyclohexane

(1) Bauer, R. K.; Borenstein, R.; Mayo, P. de; Odaka, K.; Rafalska, M.; Ware, W. R.; Wu, K. C. *J. Am. Chem. Soc.* **1982**, *104*, 4635.

(2) Uhl, S.; Krabichler, G.; Rempfer, K.; Oelkrug, D. *J. Mol. Struct.* **1986**, *143*, 279.

(3) Oelkrug, D.; Fleming, W.; Fulleman, R.; Gunther, R.; Honnen, W.; Krabichler, G.; Schafer, M.; Uhl, S. *Pure Appl. Chem.* **1986**, *58*, 1207.

(4) Wilkinson, F.; Willsher, C. J.; Johnston, L. J.; Casal, H. L.; Scaiano, J. C. *Can. J. Chem.* **1986**, *64*, 539.

(5) Kessler, R. W.; Wilkinson, F. *J. Chem. Soc., Faraday Trans. 1* **1981**, *77*, 309.

(6) Turro, N. J.; Zimmt, M. B.; Gould, I. R. *J. Am. Chem. Soc.* **1985**, *107*, 5826.

(7) Oelkrug, D.; Uhl, S.; Wilkinson, F.; Willsher, C. J. *J. Phys. Chem.* **1989**, *93*, 4551.

(8) Beck, G.; Thomas, J. K. *Chem. Phys. Lett.* **1983**, *94*, 553.

(9) Bjarneson, D. W.; Peterson, N. O. *J. Am. Chem. Soc.* **1990**, *112*, 988.

\* To whom correspondence should be addressed.